multi-Risk sciEnce for resilienT commUnities undeR a changiNgclimate
Codice progetto MUR: **PE00000005** – **I33C22006910006**

Deliverable title: Report on the performances of convection permitting models in weather generation

Deliverable ID: 8.4.2

Due date: 30 June 2025

Submission date: 30 July 2025

AUTHORS
Maria Vittoria Struglia (ENEA); Marta Antonelli (ENEA); Emanuela Pichelli (ENEA); Alessandro Anav (ENEA); Alessandro Dell'Aquila (ENEA); Sandro Calmanti (ENEA), Franco Catalano (ENEA), Giovanna Pisacane (ENEA); Gianmaria Sannino (ENEA); Franco Parodi (CIMA)

1. Technical references

Project Acronym	RETURN
Project Title	multi-Risk sciEnce for resilienT commUnities undeR a changiNg climate
Project Coordinator	Domenico Calcaterra UNIVERSITA DEGLI STUDI DI NAPOLI FEDERICO II domcalca@unina.it
Project Duration	December 2022 – November 2025 (36 months)

Deliverable No.	DV8.4.2
Dissemination level*	CO
Work Package	WP4 - Towards a regional high-resolution convection-permitting climate model for weather scenario generation
Task	T8.4.2 - Assessing the performances of the newly developed models for studying convective events
Lead beneficiary	ENEA
Contributing beneficiary/ies	UNIBO

* PU = Public

PP = Restricted to other programme participants (including the Commission Services)

RE = Restricted to a group specified by the consortium (including the Commission Services)

CO = Confidential, only for members of the consortium (including the Commission Services)

Document history

Version	Date	Lead contributor	Description
0.1	28.07.2025	Maria Vittoria Struglia, Marta Antonelli, Emanuela Pichelli (ENEA)	First draft
0.2			Critical review and proofreading
0.3			Edits for approval
1.0			Final version

2. ABSTRACT

This deliverable describes the results of the evaluation runs performed with the new models operating at a horizontal resolution that allows convective phenomena to be explicitly resolved.

Two different versions of the WRF-ARW model at a convection-permitting scale were independently developed and tested within the partnership.

The activities of Task 8.4.2 have focused on assessing the ability of the CPMs and RCMs to represent past convective events and their observed statistical properties, in order to meet the main objectives of the RETURN project as well as the needs of the impact-chain developers. This document describes the numerical simulation experiments, which constitute the deliverable of the task, and mainly shows the results of the analysis of the precipitation field, as well as the statistics of extremes produced in CPM and RCM model runs for the current climate. These are compared to benchmark datasets, including observations where available.

3. Table of contents

List of Figures

Figure 8: ENEA ERA5IT3 - Boxplots of the wet-day frequency bias of the two simulations (ERA5IT3 in pink and ERA5D02 in orange) against EURO4M for the four seasons: DJF (top-right), MAM (top-left), JJA (bottom-right), SON (bottom-left). Box edges are set at 25^{th} and 75^{th} percentiles, while black whiskers indicate the 5^{th} and 95^{th} percentile interval, and outliers at the distribution edges are shown by empty circles.

Figure 9: ENEA ERA5IT3 - Map of seasonal (DJF, MAM, JJA, SON from left to right) bias of the two simulations ERA5IT3 (top row) and ERA5D02 (bottom row) against EURO4M dataset

Figure 10: ENEA ERA5IT3 - Boxplots of the bias of the 99^{th} percentile of daily simulated precipitation (Pink ERA5IT3, orange ERA5D02) against EURO4M for the different seasons (DJF at top-right, MAM at top-left, JJA at bottom-right, SON at bottom-left).

Figure 11: ENEA ERA5IT3 - PdF of total precipitation on the alpine area: left above 1000m, right below 1000m. Intercomparison with different datasets.

Figure 12: ENEA ERA5IT3 - Diurnal Cycle of total precipitation over Italy: JJA season and wet hours

Finanziato dall'Unione europea NextGenerationEU | Ministero dell'Università e della Ricerca | Italiadomani PIANO NAZIONALE DI RIPRESA E RESILIENZA

4. Performances of newly developed convection permitting models

Increasing the spatial resolution of climate models to the scale of convection, i.e. a few kilometers, enables them to explicitly resolve convective atmospheric processes, rather than relying on parameterizations for their representation.
Within the RETURN project, climate modelling is performed at the convection-permitting scale (finer than 4 km) to produce high-resolution regional information for climate change impact assessments and to be able to represent extreme events, which are usually related to local-scale interactions.
In the context of Work Package 4 of the DS spoke, we are producing new climate simulations for the national territory at scales suitable for resolving convection. Previous milestones have seen the completion of multi-scenario climate simulations up to the year 2100 at a scale of 5 kilometers (grey zone), at which it has been found that convection was explicitly resolved due to the particular model configuration implemented, by using a cumulus parameterization scheme able to dynamically switching on and off throughout the simulation, based on the model ability to explicitly represent cumulus entrainment (Struglia et al., 2025). A description of these simulations and an analysis of the results have been provided in document D.8.4.1.
This document describes the setup and analysis of the simulations carried out at the resolution of 3 kilometers (convection-permitting scale) as follow-up of the previous applications, to be used as their benchmark and to further refine the information scale.

4.1 CHAPTER Convection-Permitting Dynamical Downscaling of ERA5 for Europe and the Mediterranean Basin

CHAPTER (Computational Hydrometeorology with Advanced Performance to Enhance Realism) is a high-resolution dynamical downscaling of the ERA5 global reanalysis. It represents a significant advancement in climate and weather modeling for Europe and the Mediterranean basin. One of its primary benefits is its cloud-resolving grid spacing of 3 km by 3 km and hourly temporal resolution for the period 1981-2022, allowing for detailed and precise simulations of atmospheric phenomena.

CHAPTER has been evaluated against state-of-the-art datasets. The comparison has been conducted on 24-hour precipitation accumulation and 2-m daily mean temperature. CHAPTER has been compared to ERA5-Land (Munoz-Sabater *et al.*, 2021) and the high-resolution precipitation dataset CHELSA (Karger *et al.*, 2021). The observational datasets used for validation are E-OBS (Cornes *et al.*, 2018), for both temperature and precipitation, and EURADCLIM (Overeem *et al.*, 2022), only for precipitation. The added value of CHAPTER over ERA5 has also been assessed.

A fuzzy verification approach, as described by Ebert (2008), is utilized to compare the precipitation performance of CHAPTER, CHELSA, and ERA5-Land. Unlike traditional nearest-point verifications that require exact matches between forecast and observation pairs, fuzzy verification relaxes matching conditions, considering factors such as spatial and temporal proximity. This approach is particularly beneficial for high-resolution models where exact matches with observations are challenging, mitigating ”double-penalty” issues (Rossa *et al.*, 2008), where forecasts may be correct but are penalized for minor spatial or temporal offsets. Three scores have been computed: the Fraction Skill Score (FSS), the Probability of Detection (POD) and the False Alarm Ratio (FAR).

For the comparison between CHAPTER, CHELSA, and ERA5-Land with E-OBS as the ground truth, all datasets perform better in autumn and winter. True events are well-represented, and the ratio of false events is low. In these seasons, the models are reliable at a spatial scale of 30 km and an intensity of 8 mm per day. The worst scores occur in summer, when the reliable intensity decreases to 5 mm per day for a spatial scale of 30 km, indicating that strong localized convective events are not well represented. The comparison of CHAPTER and CHELSA with EURADCLIM as the ground truth yields similar results.

Bias and Root Mean-Square Errors (RMSE) have also been computed for both precipitation and temperature (see Fig. 2 and Fig. 1). Compared to ERA5-Land, CHAPTER exhibits a higher positive bias in precipitation, particularly in summer over continental Europe. It is known that WRF simulations systematically show a positive precipitation bias and an overestimation of wet-day frequency (Warrach-Sagi *et al.*, 2013). Spatially, both datasets underestimate precipitation along the African coast of the Mediterranean region, while the Alps are the main area where precipitation is overestimated. However, in both regions, these biases can be partially attributed to the low density of the E-OBS network.

Regarding monthly temperature, ERA5-Land consistently shows a positive bias, while CHAPTER aligns more closely with E-OBS. Seasonal biases reveal that ERA5-Land's overestimation mainly occurs in summer and autumn, whereas CHAPTER exhibits a compensating pattern of summer overestimation and winter underestimation, explaining its better overall agreement with observations. Spatially, both datasets overestimate temperatures along the African coast and underestimate them in the Alps, which may partly be due to sparse observational data. Despite CHAPTER's lower mean bias, its RMSE is generally higher, especially in winter, indicating larger but compensating deviations from E-OBS.

The added value of CHAPTER over ERA5 has been assessed using E-OBS as the reference. The analysis, conducted at ERA5's resolution, shows that CHAPTER generally improves temperature representation across all seasons and throughout the domain. For precipitation, CHAPTER adds value in the Central European plains during autumn, winter, and spring but performs worse in summer and mountainous regions, where ERA5 aligns better with E-OBS. Discrepancies in summer and complex terrains may partly stem from E-OBS uncertainties, such as sparse station data, particularly for extreme rainfall.

CHAPTER captures intense precipitation better than ERA5 and E-OBS, especially in summer, as shown by its comparison with EURADCLIM, a finer resolved observation dataset. Figure 3 shows the probability density function of the daily accumulated rainfall of CHAPTER, ERA5, ERA5-Land and EURADCLIM on the period 2013-2022. It can be appreciated that CHAPTER has a closer agreement with EURADCLIM, especially for the strongest intensities. However, even compared with EURADCLIN, CHAPTER still tends to overestimate extremes—potentially due to both its improved convective event resolution in summer and ERA5's tendency to overestimate large-scale precipitation in winter. This results in an overall annual overestimation of precipitation. Further research is needed to confirm these findings.

In conclusion, CHAPTER matches the performance of existing state-of-the-art datasets and presents important added value by providing a rich list of three-dimensional variables, such as temperature, water vapor mass fraction, wind components (including vertical velocity), and microphysical species mass fractions. Its enhanced spatial resolution over 42 years is valuable for comprehensive physical process studies and enables a deeper understanding of severe hydro-meteorological phenomena in a changing climate.

Finanziato dall'Unione europea NextGenerationEU
Ministero dell'Università e della Ricerca
Italiadomani PIANO NAZIONALE DI RIPRESA E RESILIENZA

For instance, statistical analyses of lightning potential indices, maximum vertical velocities in updrafts, and hail statistics can be performed using CHAPTER data and compared to observational data from recent climatologies (Taszarek *et al.*, 2019; Punge and Kunz, 2016). This will enhance our understanding of the physics behind lightning and hailstorm phenomena and their predictability, as explored in Dowdy *et al.* (2020). These insights are valuable for sectors like insurance, where risk assessment and damage prediction are critical.

Moreover, CHAPTER's high-resolution reanalysis fields, when coupled with models like the Continuum hydrological model (Silvestro *et al.*, 2013), could enable detailed studies of streamflow extremes and long-term water balances (Silvestro *et al.*, 2019). This is particularly important for regions with small hydrological catchments vulnerable to severe rainfall events (Alfieri *et al.*, 2015). By simulating various components of the water cycle, CHAPTER can produce indicators of meteorological, hydrological, and agricultural drought attributes, supporting decision-making in areas heavily affected by climate variability and extremes.

High-resolution reanalysis datasets like CHAPTER are also crucial for studying wildfires, providing detailed meteorological data essential for understanding and predicting fire behavior (Resco de Dios and Nolan, 2021). CHAPTER captures fine-scale atmospheric conditions influencing wildfire dynamics, such as wind speed, humidity, and temperature variations, as well as lightning strikes (Muller *et al.*, 2020). Additionally, CHAPTER's comprehensive data can drive fire behavior models and inform forest management practices, ultimately contributing to more effective wildfire prevention and mitigation strategies, such as prescribed fires (Francos and Ubeda, 2021).

Overall, CHAPTER is a valuable resource for climate scientists, meteorologists, and stakeholders involved in risk assessment and mitigation of extreme weather events. It offers critical insights and a robust foundation for future research and applications aimed at understanding and managing weather-related hazards in the context of global warming.

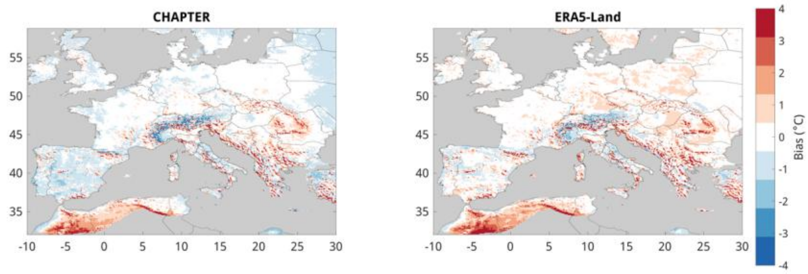

Figure 1: Bias of the daily mean temperature of CHAPTER (right) upscaled at 10 km and ERA5-Land (left) compared to E-OBS for the period 1981-2022.

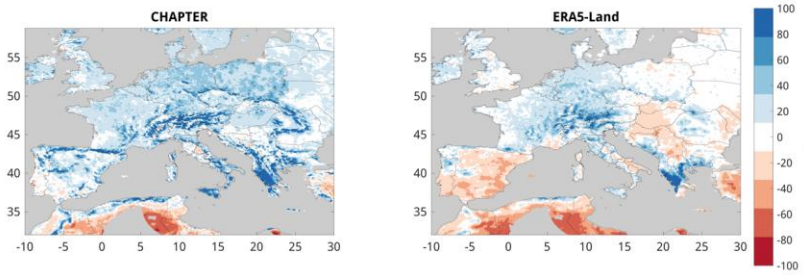

Figure 2: Bias of the daily accumulated precipitation of CHAPTER (right) upscaled at 10 km and ERA5-Land (left) compared to E-OBS for the period 1981-2022.

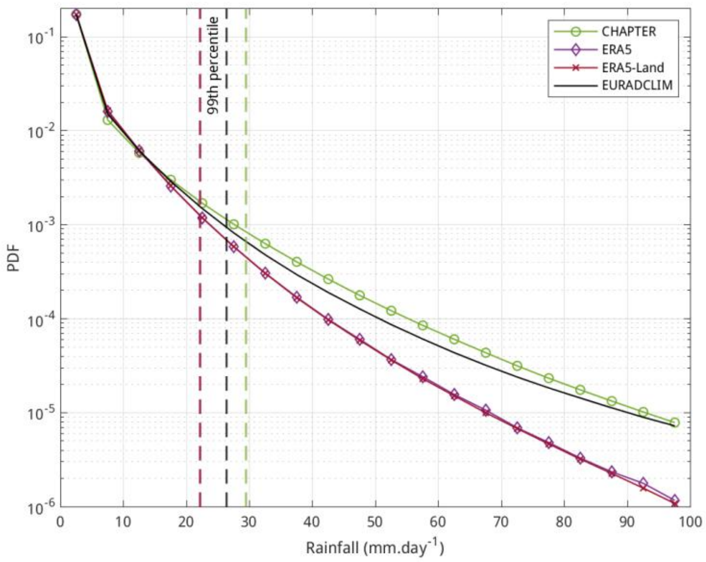

Figure 3: Probability density function of the annual daily mean precipitation for the period 2013-2022 for the datasets: EURADCLIM, ERA5, ERA5-Land, and CHAPTER.

4.2 ERA5IT3 Regional dynamical downscaling of ERA5 reanalysis at convection permitting scale over Italy

Following the same 2-level nesting approach already applied to produce the climate scenario simulations at the resolution of 5 km (Struglia et al.,2025, D8.4.1; in the following ERA5D02), we performed a hindcast simulation over a domain which covers the whole national territory at a horizontal resolution of 3 km (Figure 4). The Regional Climate Model (RCM) WRF-ARW (version 4.2.2) configuration is the same as test4 as described in deliverable D.8.4.1, where a preliminary sensitivity to sub-grid physics study was carried out to assess the best model setup (resumed in Table 1). Due to the limited sensitivity to microphysics and turbulence parameterizations in terms of standard statistics, as well as the representation of extreme events, the final configuration has been set to maximize the match with that of the simulations at 5 km. This choice favors a comparison between simulations which only differ for their grid-step and the activation of cumulus, lake and urban schemes, allowing to assess rigorously the added value of adopting the explicitly convection-permitting configuration.

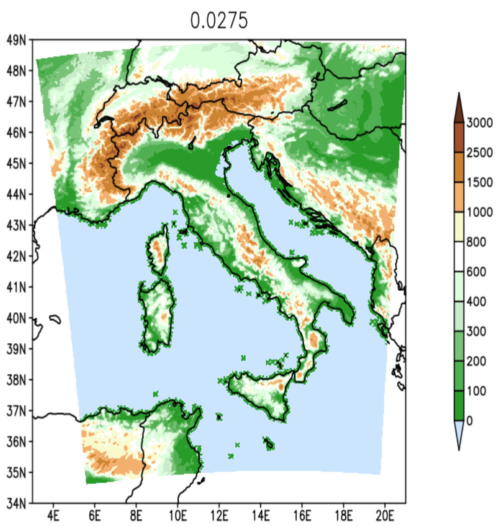

Figure 4: Model domain for the Convection Permitting version of ENEA-IT3 model

Finanziato dall'Unione europea
NextGenerationEU
Ministero dell'Università e della Ricerca
Italiadomani
PIANO NAZIONALE DI RIPRESA E RESILIENZA

Run [RES]	microphysics	PBL	surface layer	LSM	Cumulus	Lake	URB	YEARS analyzed
ERA5IT3 **[3 km]**	Thompson	MYNN	Monin-Obukhov (Janjic)	NoahMP	Off	On	On	30 (1981-2011)
ERA5D02 ~~WMED5~~ **[5 km]**	Thompson	MYNN	Monin-Obukhov (Janjic)	NoahMP	Grell-Freitas	Off	Off	30 (1981-2011)

Formattato: Inglese (Stati Uniti)

Tabella formattata

Table 1: Model parameterizations for the 3 km (ERA5IT3) and 5 km (ERA5D02) configurations

Similarly to the ERA5D02 (see deliverable D8.4.1), the ERA5IT3 domain is driven at its boundary by the 15 km simulations performed on the D01 domain (hereafter ERA5D01) over Europe. The ERA5IT3 simulation spans the period 1980-2023, but the analysis here is carried out over shorter periods. Figures 5 and 6 show the interannual variability over the PRUDENCE domain ALP ((Christensen and Christensen 2007) of the average surface temperature and total precipitation, respectively. Data are averaged over land points only. ERA5IT3 and ERA5D02 are compared with each other and benchmarked against the following datasets: ERA5, E-obs, ERA5D01 and CERRA (precipitation only).

Figures 5 and 6 show the fair representation of the interannual variability, by both ERA5IT3 (CP) and ERA5D02 (gray zone) experiments, which are very close. The CP experiment slightly further corrects the cold bias and the wet bias of the parent simulation with respect to the 5 km experiment, which in turn is simulating in a quasi-convection permitting mode, due to the use of the G-F cumulus parameterization, as extensively discussed in Struglia et al. (2025). We can here speculate that, even if with small differences, the transition to a refined CP scale still leaves room for an added value.

Commentato [EP1]: È un po' rischioso affermare questo. Perché che si stia comportando come un CPM lo sappiamo da Struglia 2025 avendo verificato che la grill si spegne. Altrimenti possiamo solo dire che hanno statistiche simili

To meet the main objectives of the RETURN project as well as the needs of the impact-chain developers, a crucial step is the assessment of the ability of the CPMs and RCMs to represent the past convective events and their observed statistical properties. To this end, in the following we focus on the seasonal analysis of the precipitation field, and on the statistics of extreme rainfalls produced by ERA5IT3 and ERA5D02 runs across the thirty-year period 1981-2011, using as benchmark high resolution observations, namely the EURO4M-APGD dataset (available from https://www.meteoswiss.admin.ch, EURO4M hereafter), which covers the Alpine area with a horizontal resolution of 5 km and available at daily temporal resolution.

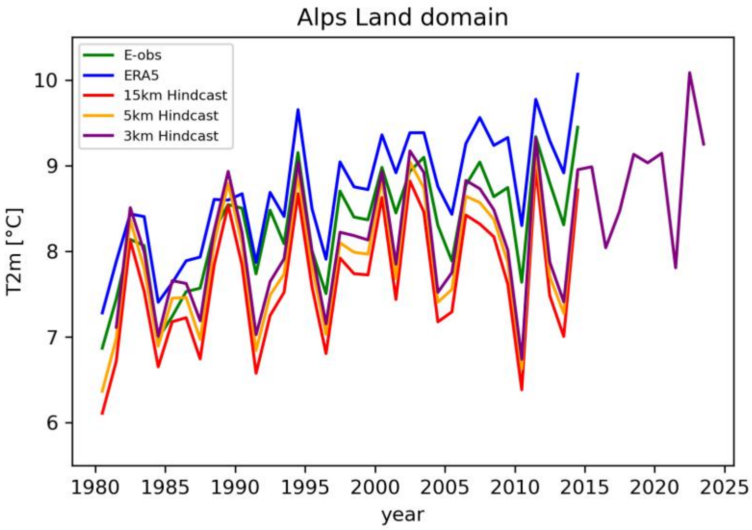

Figure 5: Mean annual surface temperature (°C) averaged over land points of the PRUDENCE ALP domain.

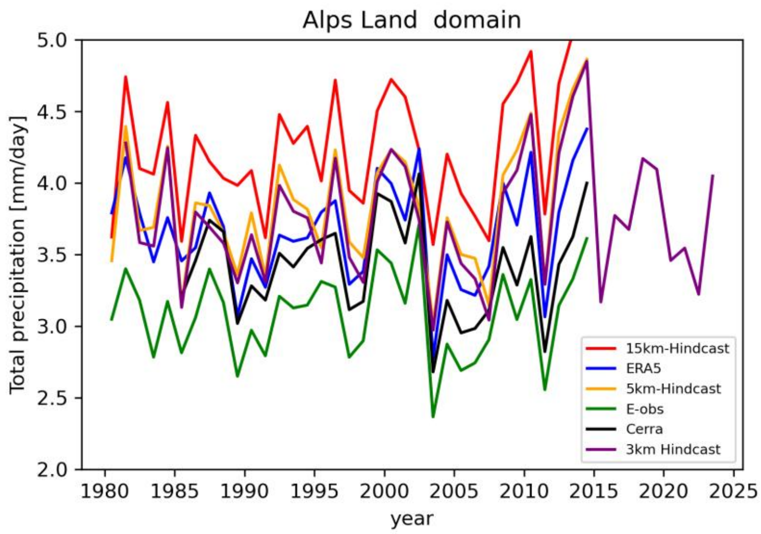

Figure 6: Mean annual daily precipitation(mm/day), averaged over land points of the PRUDENCE ALP domain.

Figure 7 shows the wet-day frequency (fraction of number of wet-days, i.e. days with at least 1 mm of rainfall, per season) for the different datasets. The figure shows EURO4M, ERA5IT3, ERA5D02 and simulations bias against EURO4M from top to bottom, across the four seasons: winter (DJF), spring (MAM), summer (JJA), fall (SON) from left to right. We note that the seasonal wet-day frequency is broadly comparable among the two evaluation experiments, however in the CP one (second row) the spatial distribution is closer to the observations (first row), especially in DJF, strongly reducing the positive bias show by ERA5D02 (third row). This tendency is confirmed in summer and fall, when convective precipitations are more likely, and especially around the highest topography.

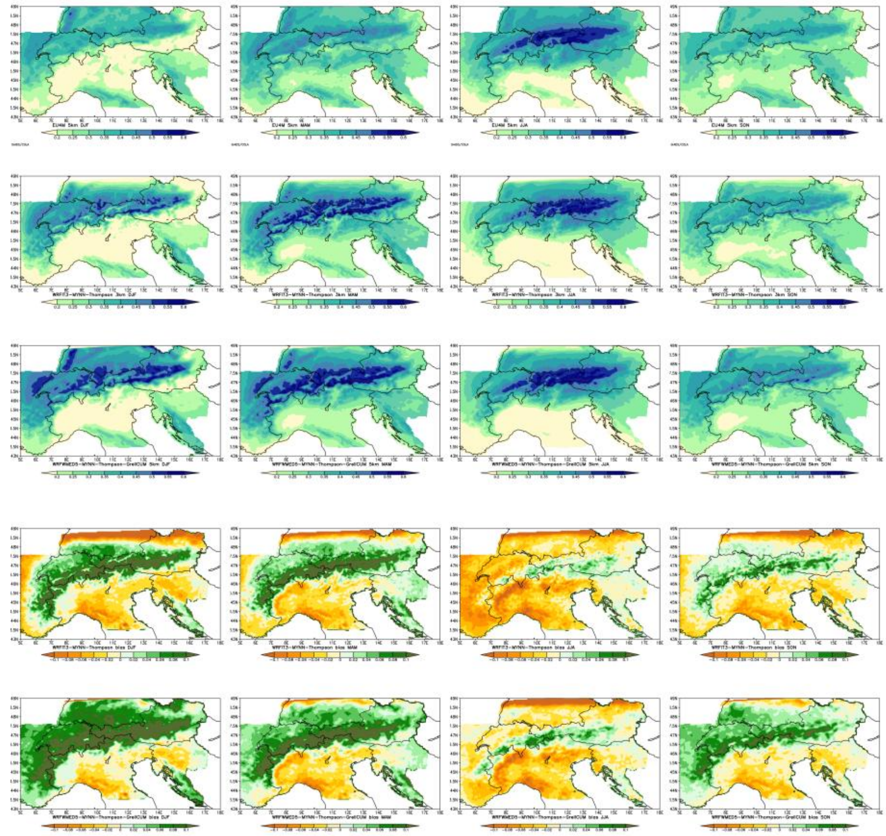

Figure 7 Wet-day frequency. From top to bottom: EURO4M, ERA5IT3, ERA5D02 (absolute values), ERA5IT3 bias against EURO4M, ERA5D02 bias against EURO4M. From left to right: DJF, MMA, JJA, SON

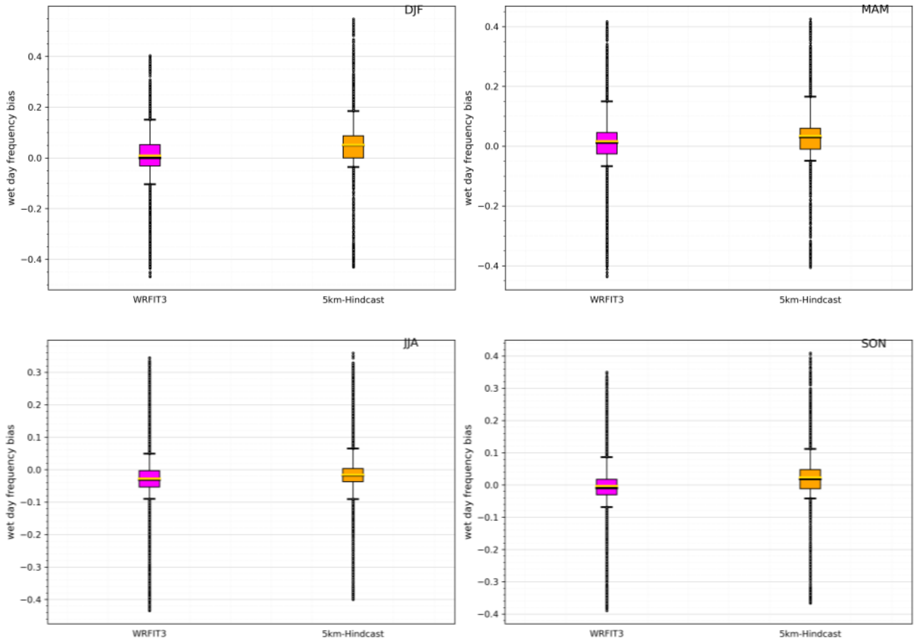

Figure 8 Boxplots of the wet-day frequency bias of the two simulations (ERA5IT3 in pink and ERA5D02 in orange) against EURO4M for the four seasons: DJF (top-right), MAM (top-left), JJA (bottom-right), SON (bottom-left). Box edges are set at 25th and 75th percentiles, while black whiskers indicate the 5th and 95th percentile interval, and outliers at the distribution edges are shown by empty circles.

Figure 8 shows the seasonal boxplots of the wet-day frequency bias of the two hindcast simulations against EURO4M across the observation area. The figure confirms the previously noted reduction of the bias but with similar spatial variability between the two simulations and except in JJA, when the improvement of the positive bias over the highest mountain reliefs is offset by the negative bias in the surrounding areas.

As shown in Fig 9 and 10, the representation of the heavy precipitation (intensity of the daily precipitation over the 99th percentile of the whole precipitation distribution) bias for ERA5IT3 and ERA5D02 against EURO4M is comparable across the observation area. The two figures show the seasonal bias maps and boxplots of the heavy precipitation, respectively. Although the mean bias is similar (Figure 9), the CP ERA5IT3 simulation produces larger extremes. This is in part confirmed by figure 11, which reports the Probability Density Functions (PdFs) of the daily precipitation for the 1981-2011 period above and below the 1000 m terrain height; the plots show longer tails for ERA5IT3 (pink) compared to ERA5D02 (orange), as well as more frequent severe hazards, especially over the mountains (Fig. 11, left panel). Although ERA5IT3 is apparently producing larger overestimation of both EURO4M (light green) and CERRA (black) than ERA5D02, we have to note that these two observed datasets have same 5km grid-step, which favors the comparison with the ERA5D02 run. Moreover, some of the events at the ERA5IT3 tail are not necessarily overestimated by the model, but rather under-caught in the rain-gauge networks, mainly true over hills or mountains (Fig. 11, left panel).

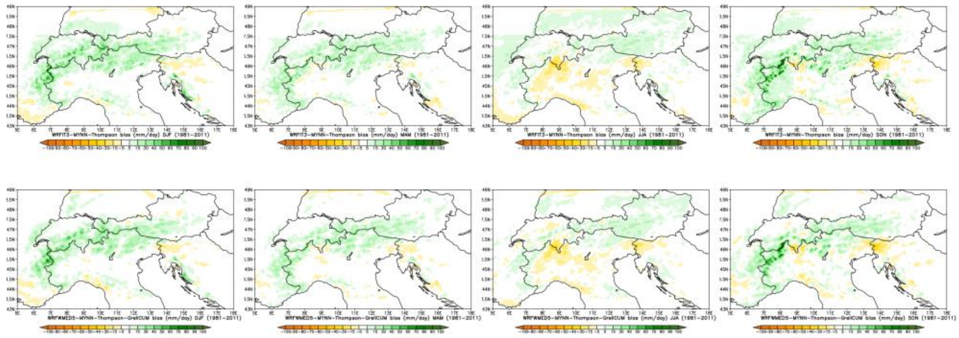

Figure 9: Map of seasonal (DJF, MAM, JJA, SON from left to right) bias of the two simulations ERA5IT3 (top row) and ERA5D02 (bottom row) against EURO4M dataset.

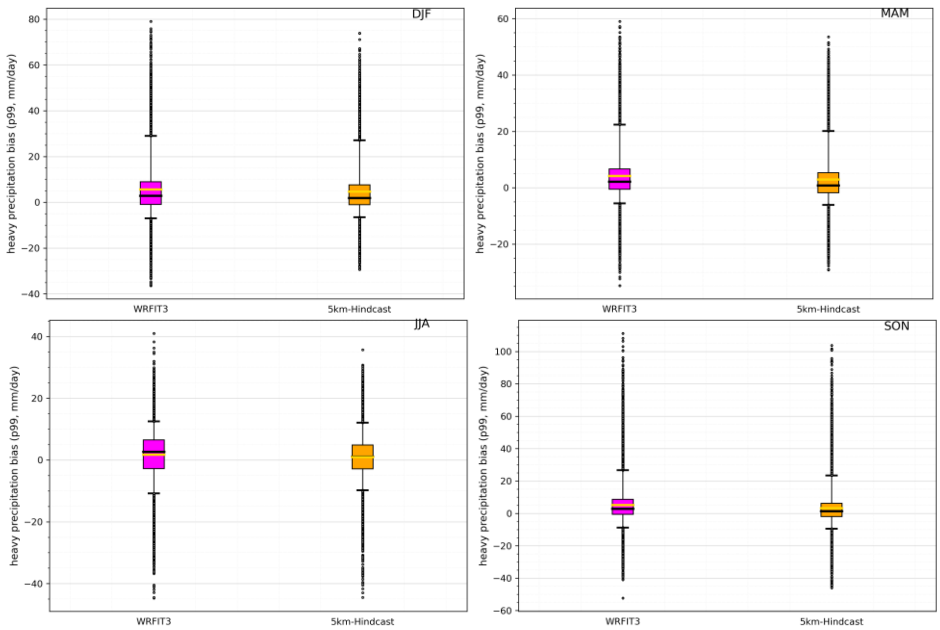

Figure 10: Boxplots of the bias of the 99th percentile of daily simulated precipitation (Pink ERA5IT3, orange ERA5D02) against EURO4M for the different seasons (DJF at top-right, MAM at top-left, JJA at bottom-right, SON at bottom-left).

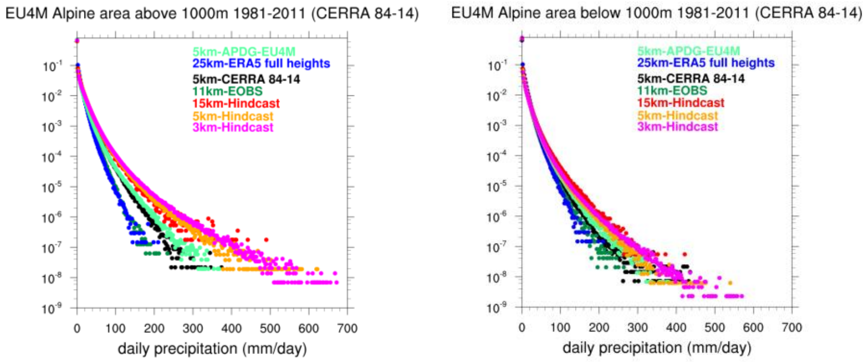

Figure 11: PdF of total precipitation on the alpine area: left above 1000m, right below 1000m. Intercomparison with different datasets.

Another significant improvement expected when using the CPM scale is the representation of the diurnal cycle. Figure 12 shows the diurnal cycle for the ERA5IT3 experiment over Italy for the years 2003–2017. Due to the lack of easily accessible and adequate observations against which to evaluate the results obtained, we refer to Fig. 12 in Giordani et al.,2023. We note that the results obtained in terms of timing of daily maxima are very similar to that obtained by the SPHERA product, which moreover is a reanalysis product rather than a simple hindcast experiment as the simulation presented here.

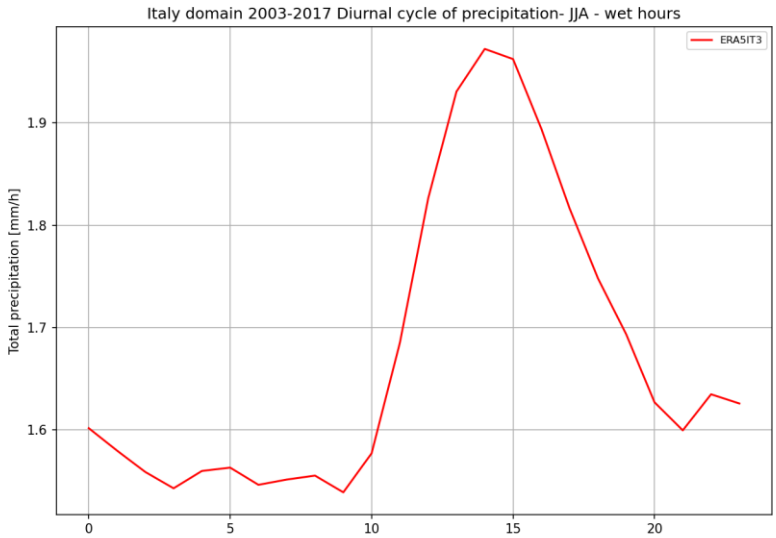

Figure 12 : Diurnal Cycle of total precipitation over Italy: JJA season and wet hours

Finanziato dall'Unione europea NextGenerationEU | Ministero dell'Università e della Ricerca | Italiadomani PIANO NAZIONALE DI RIPRESA E RESILIENZA

5. Conclusions

A numerical modelling chain to produce climate simulations at convection permitting scale has been carried out.

A protocol simulation has been defined, and its effectiveness has been proven using the ERA5 dataset as global driver. The realization of the hindcast run is of primary importance as it allows us to test the ability of the numerical instrument to reproduce the current climate by validating the system against reanalysis and observational datasets.

Results of the hindcast simulations have been shown, demonstrating the fair performances of high-resolution climate simulations either in the grey-zone or at convection permitting scale. Improvement in the temporal distribution of precipitations is especially found when resorting to CPM version of the model, both in terms of wet-day frequency and of diurnal cycle.

6. References

Alfieri, L., Burek, P., Feyen, L., and Forzieri, G. (2015). Global warming increases the frequency of river floods in Europe. *Hydrology and Earth System Sciences*, 19(5):2247–2260.

Christensen, J.H., Christensen, O.B. A summary of the PRUDENCE model projections of changes in European climate by the end of this century. Climatic Change 81 (Suppl 1), 7–30 (2007). https://doi.org/10.1007/s10584-006-9210-7

Cornes, R. C., van der Schrier, G., van den Besselaar, E. J., and Jones, P. D. (2018). An ensemble version of the e-obs temperature and precipitation data sets. *Journal of Geophysical Research: Atmospheres*, 123(17):9391–9409.

Dowdy, A. J., Soderholm, J., Brook, J., Brown, A., and McGowan, H. (2020). Quantifying hail and lightning risk factors using long-term observations around australia. *Journal of Geophysical Research: Atmospheres*, 125(21):2020JD033101.

Ebert, E. E. (2008). Fuzzy verification of high-resolution gridded forecasts: a review and proposed framework. *Meteorological Applications: A journal of forecasting, practical applications, training techniques and modelling*, 15(1):51–64.

Francos, M. and Ubeda, X. (2021). Prescribed fire management. *Current Opinion in Environmental Science & Health*, 21:100250.

Giordani, A., Cerenzia, I.M.L., Paccagnella, T., and Di Sabatino, S.: SPHERA, a new convection-permitting regional reanalysis over Italy: Improving the description of heavy rainfall. Quarterly Journal of RMS, 149, 752,781-808, https://doi.org/10.1002/qj.4428, 2023.

Karger, D. N., Wilson, A. M., Mahony, C., Zimmermann, N. E., and Jetz, W. (2021). Global daily 1 km land surface precipitation based on cloud cover-informed downscaling. Scientific Data, 8(1):307.

Muller, M. M., Vila-Vilardell, L., and Vacik, H. (2020). Towards an integrated forest fire danger assessment system for the european alps. *Ecological Informatics*, 60:101151.

Munoz-Sabater, J., Dutra, E., Agust´ı-Panareda, A., Albergel, C., Arduini, G., Balsamo, G., Boussetta, S., Choulga, M., Harrigan, S., Hersbach, H., et al. (2021). Era5-land: A state-of-the-art global reanalysis dataset for land applications. *Earth system science data*, 13(9):4349–4383.

Overeem, A., van den Besselaar, E., van der Schrier, G., Meirink, J. F., van der Plas, E., and Leijnse, H. (2022). Euradclim: the european climatological high-resolution gauge-adjusted radar precipitation dataset. *Earth System Science Data Discussions*, 2022:1–34.

Punge, H. J. and Kunz, M. (2016). Hail observations and hailstorm characteristics in europe: A review. *Atmospheric Research*, 176:159–184.

Resco de Dios, V. and Nolan, R. H. (2021). Some challenges for forest fire risk predictions in the21st century. *Forests*, 12(4):469.

Rossa, A., Nurmi, P., and Ebert, E. (2008). Overview of methods for the verification of quantitative precipitation forecasts. In *Precipitation: Advances in measurement, estimation and prediction*, pages 419–452. Springer.

Silvestro, F., Gabellani, S., Delogu, F., Rudari, R., and Boni, G. (2013). Exploiting remote sensing land surface temperature in distributed hydrological modelling: the example of the continuum model. *Hydrology and Earth System Sciences*, 17(1):39–62.

Silvestro, F., Rossi, L., Campo, L., Parodi, A., Fiori, E., Rudari, R., and Ferraris, L. (2019). Impact-based flash-flood forecasting system: Sensitivity to high resolution numerical weather prediction systems and soil moisture. *Journal of Hydrology*, 572:388–402.

Struglia, M. V., Anav, A., Antonelli, M., Calmanti, S., Catalano, F., Dell'Aquila, A., Pichelli, E., and Pisacane, G.: Impact of spatial resolution on CMIP6-driven Mediterranean climate simulations: a focus on precipitation distribution over Italy, EGUsphere [preprint], https://doi.org/10.5194/egusphere-2025-387, 2025.

Taszarek, M., Allen, J., Pucik, T., Groenemeijer, P., Czernecki, B., Kolendowicz, L., Lagouvardos, K., Kotroni, V., and Schulz, W. (2019). A climatology of thunderstorms across europe from a synthesis of multiple data sources. *Journal of Climate*, 32(6):1813–1837.

Warrach-Sagi, K., Schwitalla, T., Wulfmeyer, V., and Bauer, H.-S. (2013). Evaluation of a climate simulation in europe based on the wrf–noah model system: precipitation in germany. *Climate Dynamics*, 41:755–774.